Geochemistry Geophysics Geosystems G3

Published by AGU and the Geochemical Society

Article
Volume 12, Number 10
22 October 2011
Q10016, doi:10.1029/2011GC003663
ISSN: 1525-2027

Continents, supercontinents, mantle thermal mixing, and mantle thermal isolation: Theory, numerical simulations, and laboratory experiments

A. Lenardic
Department of Earth Science, Rice University, MS 126, PO Box 1892, Houston, Texas 77251-1892, USA (adrian@esci.rice.edu)

L. Moresi
School of Mathematical Sciences, Monash University, Clayton, Building 28, Victoria 3800, Australia

A. M. Jellinek
Department of Earth and Ocean Sciences, University of British Columbia, Vancouver, British Columbia M5S 1A7, Canada

C. J. O'Neill
Department of Earth and Planetary Science, Macquarie University, Sydney, New South Wales 2109, Australia

C. M. Cooper
School of Earth and Environmental Sciences, Washington State University, Pullman, Washington 99164, USA

C. T. Lee
Department of Earth Science, Rice University, MS 126, PO Box 1892, Houston, Texas 77251-1892, USA

[1] Super-continental insulation refers to an increase in mantle temperature below a supercontinent due to the heat transfer inefficiency of thick, stagnant continental lithosphere relative to thinner, subducting oceanic lithosphere. We use thermal network theory, numerical simulations, and laboratory experiments to provide tighter physical insight into this process. We isolate two end-member dynamic regimes. In the thermally well mixed regime the insulating effect of continental lithosphere can not cause a localized increase in mantle temperature due to the efficiency of lateral mixing in the mantle. In this regime the potential temperature of the entire mantle is higher than it would be without continents, the magnitude depending on the relative thickness of continental and oceanic lithosphere (i.e., the insulating effects of continental lithosphere are communicated to the entire mantle). Thermal mixing can be short circuited if subduction zones surround a supercontinent or if the convective flow pattern of the mantle becomes spatially fixed relative to a stationary supercontinent. This causes a transition to the thermal isolation regime: The potential temperature increases below a supercontinent whereas the potential temperature below oceanic domains drops such that the average temperature of the whole mantle remains constant. Transition into this regime would thus involve an increase in the suboceanic viscosity, due to local cooling, and consequently a decrease in the rate of oceanic lithosphere overturn. Transition out of this regime can involve the unleashing of flow driven by a large lateral temperature gradient, which will enhance global convective motions. Our analysis highlights that transitions between the two states, in either direction, will effect not only the mantle below a supercontinent but also the mantle below oceanic regions. This provides a larger set of predictions that can be compared to the geologic record to help determine if a hypothesized super-continental thermal effect did or did not occur on our planet.

Components: 12,600 words, 14 figures.

Keywords: mantle convection; supercontinent.

Index Terms: 8120 Tectonophysics: Dynamics of lithosphere and mantle: general (1213); 8121 Tectonophysics: Dynamics: convection currents, and mantle plumes.

Received 15 April 2011; **Revised** 30 August 2011; **Accepted** 30 August 2011; **Published** 22 October 2011.

Lenardic, A., L. Moresi, A. M. Jellinek, C. J. O'Neill, C. M. Cooper, and C. T. Lee (2011), Continents, supercontinents, mantle thermal mixing, and mantle thermal isolation: Theory, numerical simulations, and laboratory experiments, *Geochem. Geophys. Geosyst.*, *12*, Q10016, doi:10.1029/2011GC003663.

1. Introduction

[2] The idea that continents can insulate the mantle predates the development of plate tectonics by decades [*Pekeris*, 1935]. The idea has been refined but the different heat transfer modes in oceanic and continental lithosphere remain a key underpinning.

[3] Oceanic lithosphere is relatively short-lived attesting to the fact that it is the active upper thermal boundary layer of mantle convection [e.g., *Turcotte and Oxburgh*, 1967]. Its thermal structure has thus been modeled within a thermal convection framework [e.g., *Parsons and Sclater*, 1977; *Parsons and McKenzie*, 1978; *Stein and Stein*, 1992]. Unlike oceanic lithosphere, the longevity of continental crust, and deeper continental lithosphere [e.g., *Boyd et al.*, 1985], has lead to continental thermal structure being treated within a thermal conduction framework [e.g., *Pollack and Chapman*, 1977; *Morgan and Sass*, 1984; *Rudnick et al.*, 1998]. The inefficiency of conduction, as compared to convection, leads to the idea that continents can inhibit heat loss from the mantle, i.e., act as thermal insulators. The greater thickness of continental versus oceanic lithosphere [e.g., *Jordan*, 1981] further feeds into the potential insulating effect of continents, as does their enrichment of heat producing elements [*Whitehead*, 1972; *Busse*, 1978].

[4] Starting with *Pekeris* [1935] and continuing into the post plate tectonics era [*Anderson*, 1982], the prevailing line of thought has been that continental insulation should be most pronounced during times of supercontinent assembly due to the fixity of supercontinents for extended periods of time together with their large surface areas. This idea was at the core of numerical simulations that modeled drifting continents above a convecting mantle [*Gurnis*, 1988]. Those simulation showed episodes of supercontinent assembly that lead to thermal anomalies below a supercontinent. Subsequent to that pioneering work, a wave of studies explored models of continents above a convecting mantle with added levels of complexity [e.g., *Zhong and Gurnis*, 1993; *Lowman and Jarvis*, 1993, 1995; *Guillou and Jaupart*, 1995; *Lenardic and Kaula*, 1995, 1996; *Lowman and Gable*, 1999].

[5] Although it is agreed that continents can effect mantle dynamics, the degree of any temperature increase that might occur below a supercontinent, due to continental insulation, is not agreed upon. If the temperature increase leads to mantle melting that would not occur without the insulation effect, then the effect is significant. *Coltice et al.* [2007, 2009] have used numerical simulations to argue that this is the case. At the other side of the discussion, *O'Neill et al.* [2009] and *Heron and Lowman* [2010] have used similar numerical simulations to argue that this is not the case. Their simulations lead to small temperature increases below a supercontinent. That is, the average potential temperature below a supercontinent was insignificantly different from that below oceanic domains. Thus, melting could occur only by mantle plumes that rise below the supercontinent. The idea that the dominant cause of a temperature rise below a supercontinent is due to rising mantle plumes, as opposed to continental insulation, is also inherent to the modeling studies of *Zhong et al.* [2007] and *Zhang et al.* [2010]. These authors concluded that a subcontinental mantle temperature increase below Pangea was caused by upwelling mantle plumes that formed below the supercontinent in response to circum-continental subduction zones (the circum-continental downflow associated with subducting slabs would drive upflow below the supercontinent via simple mass conservation). Insulation effects within the models were minor in comparison to temperature changes driven by upwelling plumes. Indeed, the models of *Heron and Lowman* [2010] build off of the earlier *Zhong et al.* [2007] study. *Heron and Lowman*

[2010] argue that subduction around a stagnant oceanic plate would also drive upwelling plumes. That is, if this is indeed the main factor that drives heating below a supercontinent, then the cause is not continental insulation; the effect does not actually require a continental plate, just a plate rimmed by subduction zones. It also follows that if this is the case, major subcontinental heating events should not occur in models that do not allow for plumes. Yet the models of *Coltice et al.* [2007, 2009], which do show significant heating below supercontinents, are purely internally heated so plumes can not be invoked to explain the results of these authors.

[6] Clearly the modeling efforts of various groups are providing results that are, at face value, not compatible. Reconciling these differing model results would provide deeper insights into the dynamics of continent-mantle interactions and, more specifically, into the range of mantle responses during episodes of supercontinent assembly and dispersal. We start with the position that both views are correct, in different limits, and use a combination of thermal network theory, numerical simulations, and laboratory experiments to provide tighter physical insight into the thermal link between continents and the mantle. In doing so, we gain added insight into how any supercontinent heating event would effect the entire Earth system.

[7] Our analysis will make a break from a prevalent view in the literature on super-continental insulation. It is often assumed that an insulation driven increase in mantle temperature occurs only during supercontinent episodes. We will argue that this is not correct. If continental lithosphere can insulate the mantle then it can do so with dispersed and/or drifting continents. The mantle can still have one single potential temperature if it is thermally well mixed. That is, the insulation effect of continents is global in this situation. Taking this as the reference state means that the mantle always runs hotter then it would if insulating continents were not present. The physical picture of what occurs during a transition to a supercontinent state, that is associated with a rise in subcontinental mantle temperature, then becomes distinctly different from the more traditional view. The mantle temperature below a supercontinent can rise if thermal mixing between the subcontinental and suboceanic domains is inhibited. Subduction zones circling a supercontinent provide a means to inhibit lateral mixing of subcontinental and suboceanic thermal domains. The insulating effect of continental lithosphere can then no longer be communicated to the suboceanic mantle. As a result the mantle temperature below suboceanic domains decreases while the temperature below a subduction rimmed supercontinent increases in a manner that leads to no appreciable change in the volume averaged temperature of the entire mantle. We refer to this as a thermally isolated regime to denote the strongly reduced interaction between subcontinental and suboceanic thermal domains. Transition between the two regimes involves no overall heating or cooling of the mantle as a whole. This means that the time scale of a mantle temperature increase below a supercontinent will not depend on the time scale of internal heat generation. As the transition is associated with reduced thermal mixing between mantle domains, the pertinent timescale will be an advective one which is considerably faster. A further implication is that if the mantle below a supercontinent is not thermally isolated from the suboceanic mantle, then there will be no change in the mantle temperature below it. Thus, not all supercontinent events need be associated with changes in the thermal structure of the mantle. In terms of reconciling different modeling results, an equivalent statement is that numerical simulations with continental lithosphere of equal insulating potential can lead to significant thermal changes in the mantle during supercontinent episodes as well as to no significant thermal changes during supercontinent episodes. The next section formalizes and tests these ideas.

2. Theory and Numerical Simulations

[8] We build on a body of theoretical, numerical, and laboratory work in which we have been involved [*Lenardic and Moresi*, 2001, 2003; *Cooper et al.* 2004, 2006; *Lenardic et al.* 2005; *Jellinek and Lenardic*, 2009]. These studies did not focus on supercontinents but the work can be extended to address the debate noted in the introduction. Our theoretical scaling approach is presented in Appendix A [*Lenardic and Moresi*, 2001, 2003; *Lenardic et al.*, 2005]. We have extended the theory to cover the potential that one of two different dynamic states can exist during supercontinent assembly. One state leads to a large temperature difference between subcontinental and suboceanic domains where as the other does not.

[9] We model the solid Earth heat transfer system as a thermal network comprised of oceanic and continental heat transfer paths (Figure 1a). The linking of these paths and how it effects local and global heat transfer is a main physical aspect we will focus on. The thermal network contains three

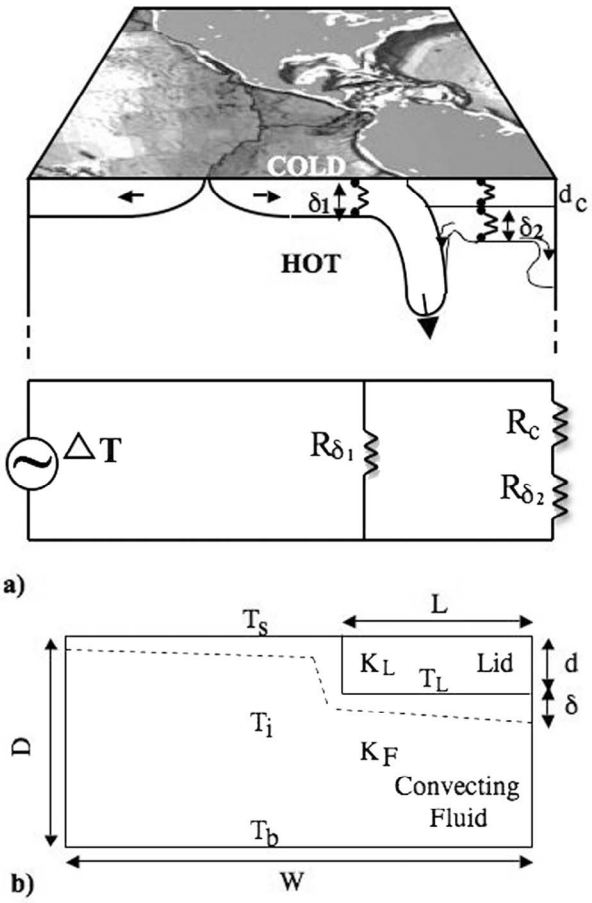

Figure 1. (a) Diagram of the solid earth thermal system, along with a thermal network analogy of the system. (b) Cartoon of a simplified thermal model that retains key elements of the solid earth thermal system.

resistive components and either one or two driving temperature drops. One component is the long lived, chemically stabilized portion of the continental lithosphere (the conducting lid composed of continental crust and depleted, chemically buoyant lithosphere). This component is linked in series with a resistance component associated with the lower mantle portion of the continental lithosphere. This is a dynamic thermal sublayer and is the active portion of the mantle thermal boundary layer below continents. Its thickness, and therefore its effective thermal resistance, is determined by the vigor of convection in the mantle and by the properties of the conducting lid [e.g., *Cooper et al.*, 2004]. Similarly the thickness of the oceanic thermal lithosphere is determined by the dynamics of mantle convection (e.g., all other factors remaining equal, enhanced convective vigor leads to a thinner oceanic lithosphere and a lower thermal resistance across the oceanic path).

[10] The concept of a thermally well mixed mantle will be crucial to our analysis. In a vigorously convecting system the average internal temperature of the convecting layer tends toward a single value with any lateral temperature variations occurring only in response to upwelling or downwelling thermal boundary layer instabilities [*Turcotte and Oxburgh*, 1967; *Turcotte and Schubert*, 1982]. This holds for a system with a single convection cell or multiple cells (it is independent of mixing within a cell versus cross cell mixing). The notion of a single mantle potential temperature stems directly from the idea that convection in the mantle is vigorous such that the mantle is thermally well mixed (this idea should not be confused with chemical mixing). A thermally well mixed mantle leads to only one bulk average internal temperature with any lateral temperature variations associated only with relatively narrow sinking slabs and upwelling mantle plumes. If super-continental insulation events can occur then this reference, thermally well mixed state must break down as, by definition, the mantle potential temperature below a supercontinent would need to be greater than the potential temperature in other regions of the mantle. This would set up a lateral temperature variation in the mantle. As such, the level of lateral mixing in the mantle is critical to the issue at hand. A large, long-lived temperature rise below a supercontinent requires that lateral thermal mixing be inhibited (within a single cell or across multiple cells). If it is not, then any thermal anomaly that may form below a supercontinent would become thermally mixed with the bulk of the mantle and a single potential temperature would be established.

[11] For our analysis, the discussion above leads to the idea that if efficient lateral mixing occurs within the mantle, then there is only one driving temperature drop, i.e., the average internal mantle temperature minus the surface temperature. If lateral mixing is inhibited then the oceanic and subcontinental mantle temperatures can differ and two driving temperature drops need to be considered. The cartoon of Figure 2 shows conceptually how we solve for the driving temperature drops in the case of poor lateral mixing or the total system temperature drop in the case of efficient lateral mixing. For either case we must solve for the internal mantle temperature in the limit of a continental lid covering the entire system. This follows from *Lenardic and Moresi* [2001]. The other end member case of no continental lid comes from classic scalings of infinite Prandtl number convection or any preferred scaling from mantle con-

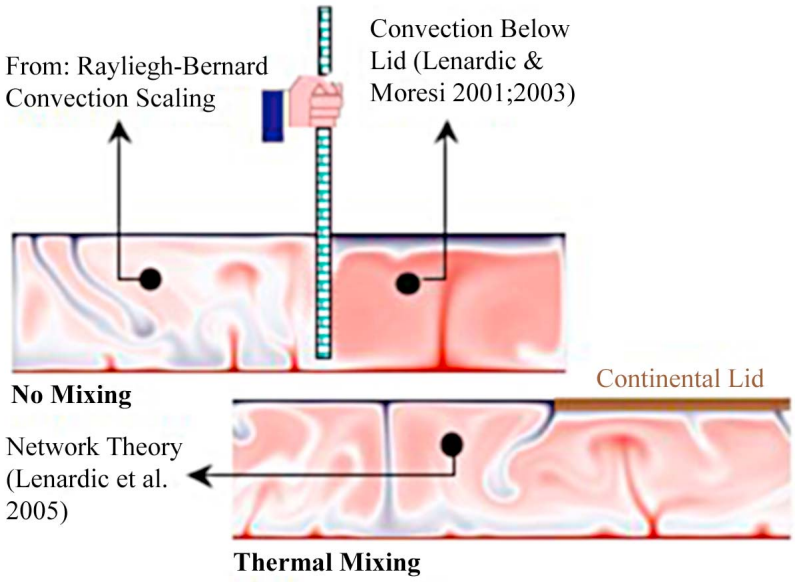

Figure 2. A schematic showing the conceptual basis of our solution procedure for determining average internal mantle temperatures in the isolated and the thermally well mixed regimes.

vection models that do not treat continents. How those two end members are linked now becomes a key issue.

[12] For poor lateral mixing, the internal temperature scalings allow us to solve for local mantle heat flux below oceans and continents. The total system heat flux becomes the surface area weighted average of the two (Appendix A). For the case of efficient lateral mixing, the theoretical scaling is a bit more involved. The continental series resistance is linked in parallel with the resistance component associated with the oceanic lithosphere and a composite thermal resistance is derived. Together with the internal temperature, which is the weighted average of the two end members, this allows us to solve for surface heat flux (Appendix A).

[13] Our numerical work to date has used simulations to confirm the scaling ideas for efficient lateral mixing [*Lenardic and Moresi*, 2003; *Lenardic et al.*, 2005]. The simulations in the right column of Figure 3 provide an example. All of the simulations of Figure 3 are purely bottom heated with a constant viscosity. The wrap around boundary conditions at the sides of the modeling domain for the right column simulations of Figure 3 allow the mantle flow field to move freely relative to the continent which leads to efficient lateral mixing and a singular mantle potential temperature. Allowing continents to drift above the mantle leads to a similar well mixed state with a mid depth mantle temperature profile that shows no lateral variations away from subducting slabs or rising plumes [*Cooper et al.*, 2006]. Figure 4a compares scaling theory predictions to a suite of simulation results in the well mixed state.

[14] The simulations in the left column of Figure 3 are designed such that the mantle flow pattern does not move relative to the continental lid. Together with the fact that the mechanical condition the convecting mantle feels at the base of the lid is rigid, as compared to the free slip condition elsewhere, this inhibits lateral thermal mixing. A thermal anomaly forms below the lid as a result and its extent tracks the extent of the lid itself. Figure 4b compares scaling theory predictions to a suite of simulation results in this alternate state.

[15] In the isolated state there is limited mixing from the continent to the ocean side within a single convection cell. If an isolated state held globally in the mantle then all convective cells would remain locked to continents and the temperature below any single continent would depend on its depth and lateral extent and not on the global continental coverage. This is consistent with the results from an alternate theoretical treatment based on a thermal loop model [*Phillips and Coltice*, 2010]. The nature of that approach means continents are assumed to remain fixed relative to a mantle convection cell. Thus, that analysis is in line with the assumption of an isolated state within our analysis.

[16] Figure 5 shows three simulations that include internal mantle heating for different continental configurations. The basal heating Rayleigh number

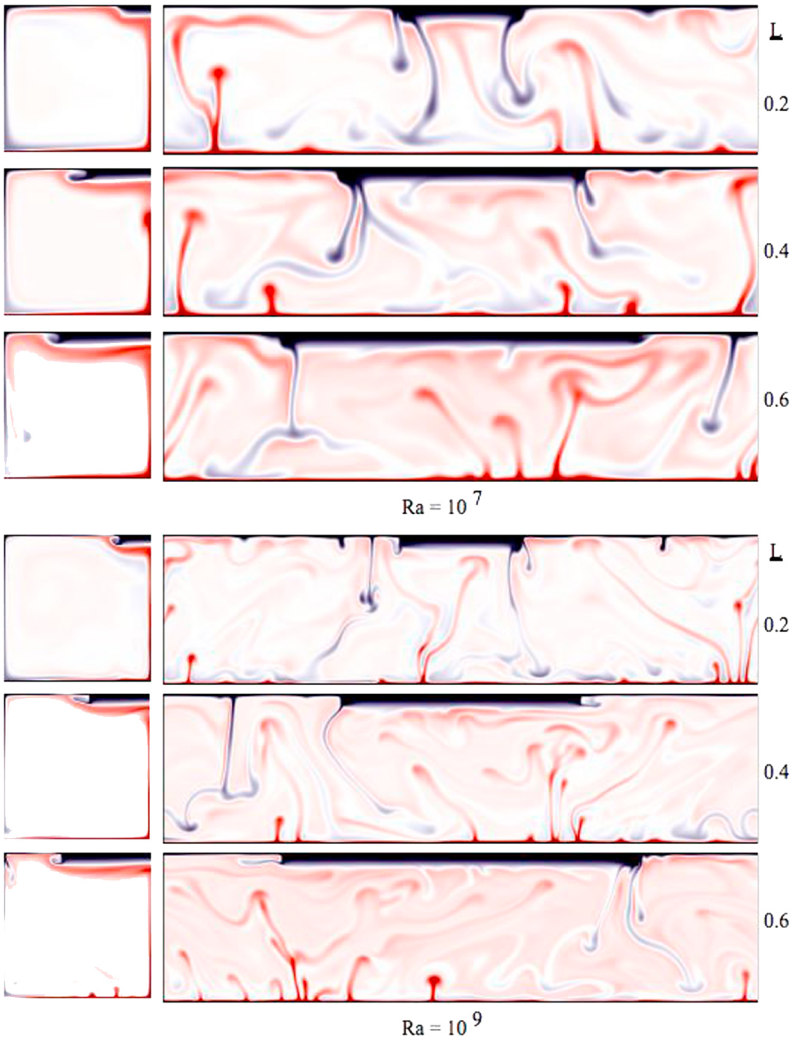

Figure 3. Numerical simulations of thermal mantle convection with variable extents of conducting continental lithosphere (L). The depth of the stable, conducting portion of the continental lithosphere is 0.076 in all cases. The 1 × 1 simulations to the left have free slip side boundary conditions which allows the convective flow to remain fixed relative to the continent. The 4 × 1 simulations to the right have wrap-around side boundary conditions which allows the mantle flow to move relative to the continent. The numerical resolution for the lower Ra cases shown is 64 × 64 elements over every 1 × 1 patch of the domain. The higher Ra cases shown have 128 × 128 elements over every 1 × 1 patch. Convergence testing was preformed on selected cases to insure that results are well resolved. The testing involved increasing resolution cases from 64 × 64 to 96 × 96 to 128 × 128 to 192 × 192 to 256 × 256 elements (see also *Lenardic and Moresi* [2003] for added discussion on resolution testing).

for the simulations is 3×10^6. The internal heating Rayleigh number is 10^7 (see Appendix B for the full conservations equations which show how mixed heating is incorporated into the models). The boundary conditions allow for efficient thermal mixing in all these simulations. For all cases there is a well defined average internal mantle temperature and the only lateral variations that occur are due to sinking or rising boundary layer instabilities. The average mantle temperature depends on the total surface area of continents and not on whether the continents are clumped together as a supercontinent or dispersed. That is to say, continents always insulate the mantle but in the well mixed state they do so globally. Although there is no localized thermal anomaly below any continents, the internal mantle temperature does depend on global continental coverage. Thus, in the well mixed state the temperature below any single continent depends on the global continental coverage and not on the extent of that specific continent. This is distinctly different from the isolated state as discussed in the previous paragraph and as mapped in more detail by *Phillips and Coltice* [2010]. In

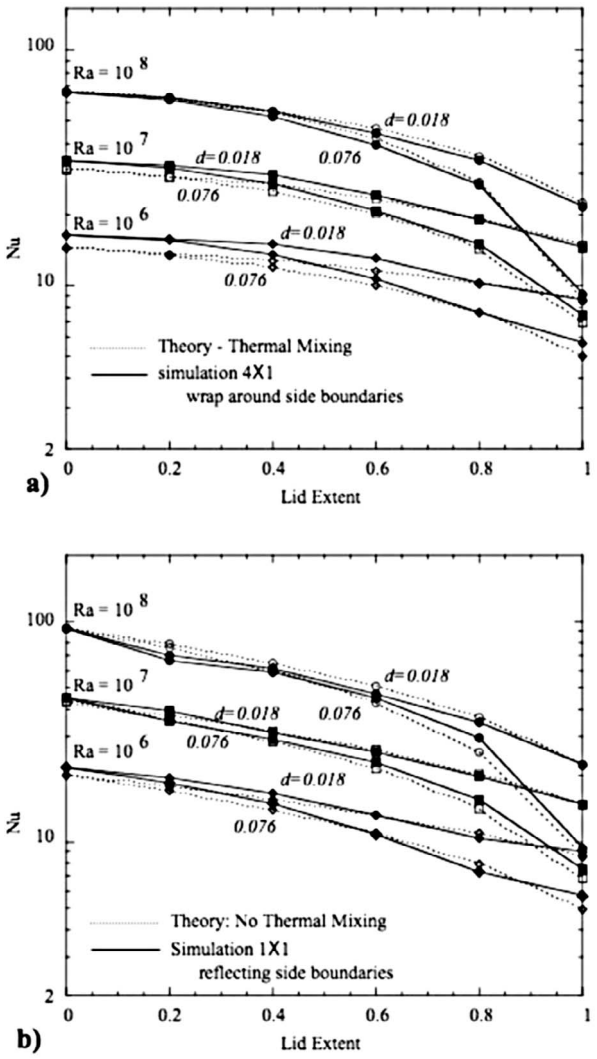

Figure 4. A comparison of scaling predictions and simulation results for Nusselt versus non-dimensional surface area of continental lid coverage for several Rayleigh number values and two different continental lid thicknesses. (a) Thermal mixing theory predictions compared to results from simulation that allow continents and large scale mantle flow to move relative to each other. (b) Thermal isolation theory predictions compared to results from simulations that have the large scale mantle flow pattern remain fixed relative to continental position.

addition to the cases shown in Figure 5, we also ran a three continent case. The mantle potential temperature remained unchanged compared to the 1 and 2 continent cases (all cases having the same total continental area), consistent with our scaling predictions for the thermally well mixed state. An earlier study [*Lenardic and Moresi*, 2003] explored six different continental configurations, for constant total continental area, in smaller modeling domains. The results were consistent with our predictions for the thermally well mixed state provided the extent of any single continent did not approach the thickness of the upper thermal boundary layer.

[17] We now consider a transition from a well mixed to a thermally isolated state. In the isolated state, our ideas predict that the insulation effect of continental lithosphere should become local which would lead subcontinental temperature to increase and suboceanic mantle temperature to decrease. The changes in terms of the network model are shown in Figure 6. A prediction from our scaling theory (Appendix A) is that the average temperature of the entire mantle should remain constant. Figure 7a shows the time evolution of a simulation that allows for a regime transition by imposing conditions that generate subducting slabs at both sides of a supercontinent (in effect, the slab curtains prevent lateral mixing). Figure 8a shows mid-mantle temperature profiles at two times and 8b shows the suboceanic and subcontinental averages over time. The average temperature of the entire mantle remains constant to within 2–3% over the transition between the two sates.

[18] Figure 7b shows a time slice from a simulation that started with the initial state of Figure 7a but changed the side boundary conditions from wrap-around to reflecting. This allowed a long wavelength cell to form and remain fixed relative to the continent. This inhibited lateral mixing allowing a lateral temperature gradient to develop in the mantle. The degree of thermal isolation between the subcontinental and suboceanic mantle domains was not as complete as for the case with a subduction curtain at the same model evolution times. None the less, the average mid mantle depth temperature increase below the continent in Figure 7b was still significant; 4% versus 6% for the subduction curtain case at an equivalent evolution time.

[19] Figures 7 and 8 show that the extent of temperature variations in the thermally isolated regime greatly exceeds the lateral dimension of mantle upwellings. That is, mantle plumes are not the cause of the subcontinental temperature increase in the simulations. To make this clear, we have performed simulations that are purely internally heated (Figure 9). Our scaling theory predicts that the mantle temperature below a continent in the thermally isolated regime depends on the thickness of a continent, its thermal conductivity, and the mantle Rayleigh number (equations (A9) and (A10) of Appendix A). The lower mantle boundary layer does not enter directly. The mantle runs hotter as a result of insulation from the continent and this

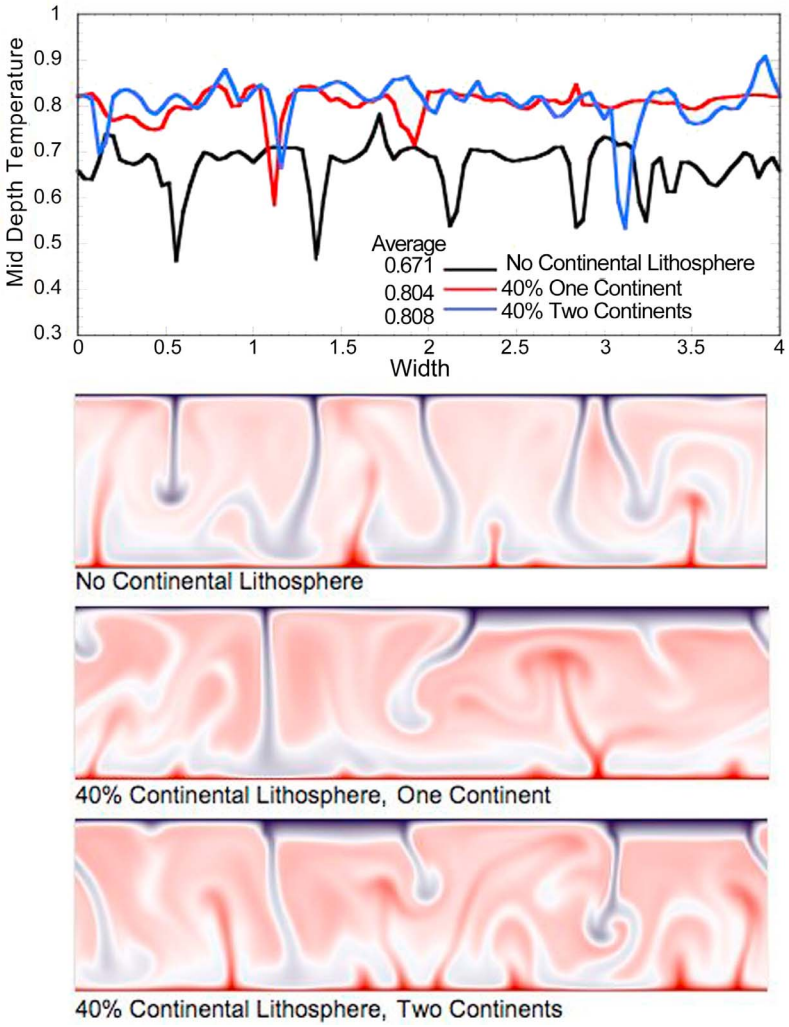

Figure 5. (top) Mid-depth mantle temperatures from (bottom) three numerical simulations that are all characterized by efficient lateral mixing within the convecting mantle.

does not depend on the heating mode of the mantle. If continental lithosphere leads to a thicker upper boundary layer then would result without it, then a purely internally heated mantle will heat up so that surface heat flow balances internal heat production. If the isolated regime breaks down, then the overall mantle temperature should still remain constant, i.e., it should be the volume average of the suboceanic and subcontinental domains in the isolated regime. Conversely, going from a thermally well mixed to an isolated regime should lead subcontinental/suboceanic mantle temperatures to increase/decrease in a manner that does not alter the average temperature of the entire mantle. As the transition is associated with cutting off advective mixing between domains, the time scale for significant changes to occur should be comparable to a mantle overturn time. The simulations of Figure 9 confirm these predictions and, together with our purely bottom heated and mixed heating simulations, show that our main results are, to first-order, independent of mantle heating mode. This allows us to connect our ideas to the simulations of *Coltice et al.* [2007] which assumed an internally heated mantle.

[20] Figure 10 compares our predictions to the simulation results of *Coltice et al.* [2007]. As the two continents in that simulation come together to form a supercontinent, the average temperatures below subcontinental and suboceanic domains change. These changes are captured by our theory for a transition from a mixed to a thermally isolated state.

[21] Our simulations and those of *Coltice et al.* [2007] show that a significant temperature increase can occur within 100 my below a thermally isolated

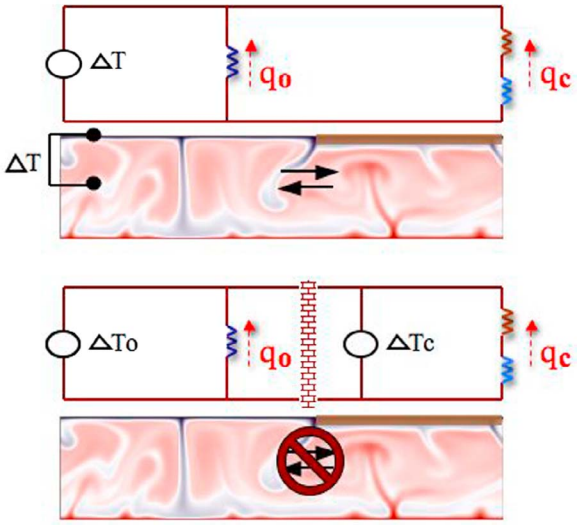

Figure 6. Cartoon showing how cutting off lateral mixing between subcontinental and suboceanic mantle would effect out thermal network model.

supercontinent. This time scale is rapid compared to the time scale for conduction across the mantle or continental lithosphere and/or the time scale associated with heating due to decay of radiogenic elements in the mantle [e.g., *Lowman and Gable*, 1999; *Zhong et al.*, 2007]. The main factor that allows for the transition is suppression of lateral mixing, the time scale for which is comparable to the mantle overturn time. The reduction in the length scale of overturning motions in the isolated regime, due to confinement of the two domains, further reduces the time scale required for significant thermal changes to occur. The fact that the changes in mantle temperature are due to suppression of lateral mixing is also why the thermal effects are felt in the suboceanic and subcontinental mantle over the entire mantle depth (as opposed to just locally below a supercontinent). Even though the transition between states leads to significant temperature changes over 100 my, the time scale for the system to reach a new statistically steady state approaches 1 Gy (Figure 8b). The implication is that if a transition did occur, then from the time of supercontinent assembly to dispersal the mantle would not be in a statistically steady state. That is, the assumption of statistical thermal equilibrium would not hold even though the average global temperature of the mantle was not changing.

[22] Allowing for more complex rheologic behavior, that more accurately models oceanic plates, does not change our main results (Figure 11). These simulations have a strongly temperature-dependent viscosity. The temperature-dependence allows for a six-order of magnitude viscosity variation in the mantle (see Appendix B for the specific viscosity function). This strong temperature-dependence of mantle viscosity does not lead to an appreciable change in the evolution of suboceanic and subcontinental mantle temperatures during a transition from a well mixed to a thermally isolated state (Figure 11b). The changes in mantle potential temperatures coupled to a temperature-dependent viscosity allow for an enhancement of some of the key effects predicted by our scaling theory (Appendix A). In the well mixed state, the presence of continents influences the heat loss from oceanic regions by raising the mantle potential temperature. For a temperature-dependent viscosity this has an enhanced effect on increasing the effective Rayleigh number driving convection. Thus, oceanic plate overturn and associated heat loss are greater than they would be without continents and without thermal mixing. For the thermally isolated state the prediction is that the potential temperature below oceanic regions should drop, viscosity should increase, and the rate of oceanic plate overturn and associated local heat loss should drop. The heat loss from oceanic regions dominates global heat loss which leads to that added prediction that global mantle heat loss should be lower in the isolated relative to the well mixed state. Our numerical simulation bear out this expectation. The global heat loss in the well mixed simulation is 9% higher than that from the thermally isolated simulation.

[23] The simulations of Figure 11 also incorporate a depth-dependent mantle rheology with a higher lower mantle viscosity. Depth-dependence increases the potential for long wavelength convection [*Bunge et al.*, 1996; *Zhong et al.*, 2000; *Busse et al.* 2006; *Lenardic et al.*, 2006; *Hoink and Lenardic*, 2008, 2010]. This becomes prominent for the middle simulation of Figure 11a. For that simulation, thermal isolation results from a long wavelength mantle convection cell becoming fixed relative to a supercontinent. In our 2D models this is achieved by imposing reflecting side boundary conditions. If the side boundary conditions are re-set to wrap around, as per the top simulation of Figure 11a, then the long wavelength cell could not persist. However, in a fully 3D spherical case the pattern could remain fixed relative to the supercontinent if it was associated with a degree one flow. The dimensions of the single cell in the middle simulation of Figure 11a are comparable to the cell extent needed for a degree one flow. As well as facilitating long wave flow, the depth-dependence enhances isolation effects. That is, the high vis-

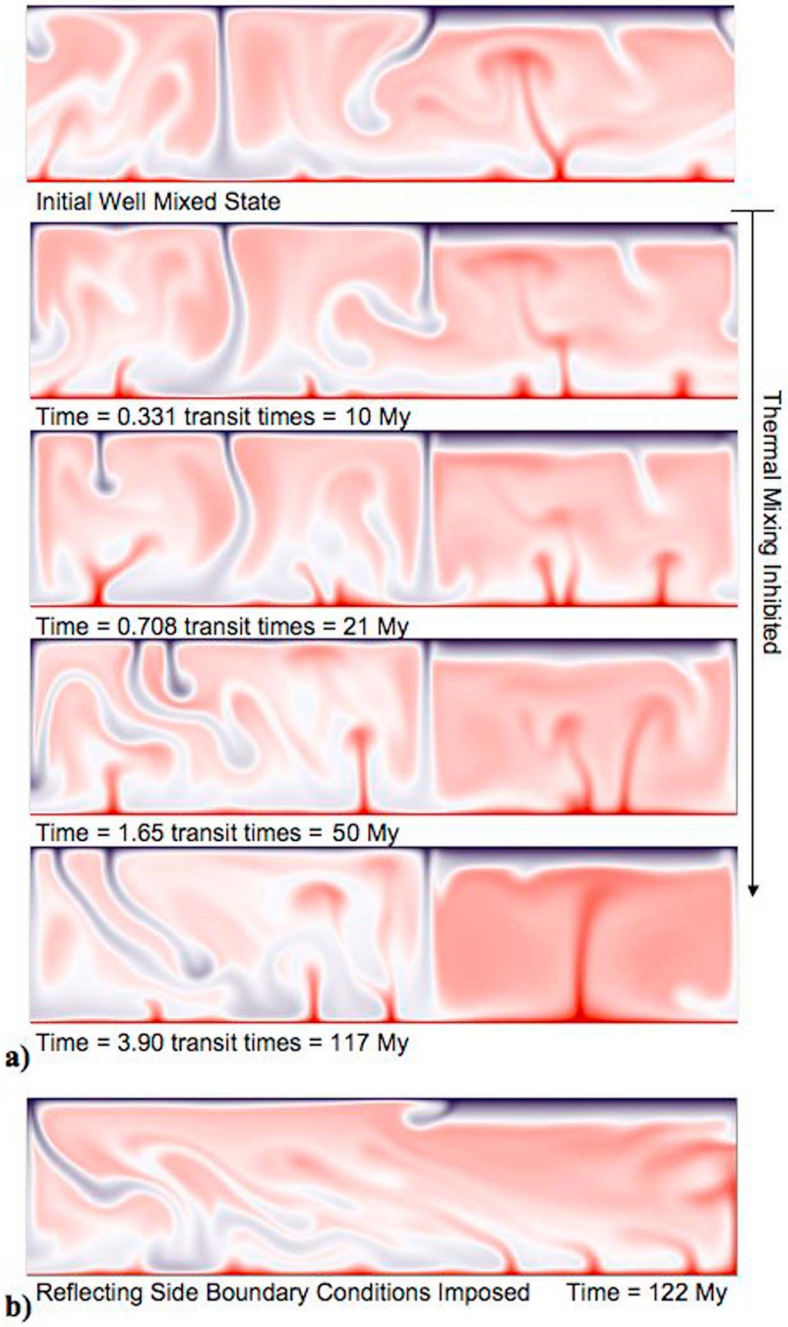

Figure 7. (a) Temporal evolution of a numerical simulation that transitions from a thermally well mixed to a thermally isolated regime. The transition is initiated by fixing the side boundary conditions to be free-slip, reflecting versus wrap-around and by initiating a peripheral mantle down flow at the edge of the model supercontinent. This was achieved by prescribing a zero horizontal flow condition at the continental edge over a depth extent of 0.8. The sinking velocity of the down flow is not prescribed but is a function of the system dynamics. The transit time is the time it would take a mantle parcel to move from the top to the bottom of the system based on the rms velocity of the simulation. The scaled time assumes whole mantle depth and a mean mantle convection velocity of 10 cm/yr. (b) A time frame from a simulation that imposed reflecting side boundary conditions versus wrap-around boundary conditions. This resulted in a transition to a partially isolated regime as it lead to a large scale mantle flow pattern that remained fixed relative to the supercontinent above it (as per the left side simulations of Figure 3).

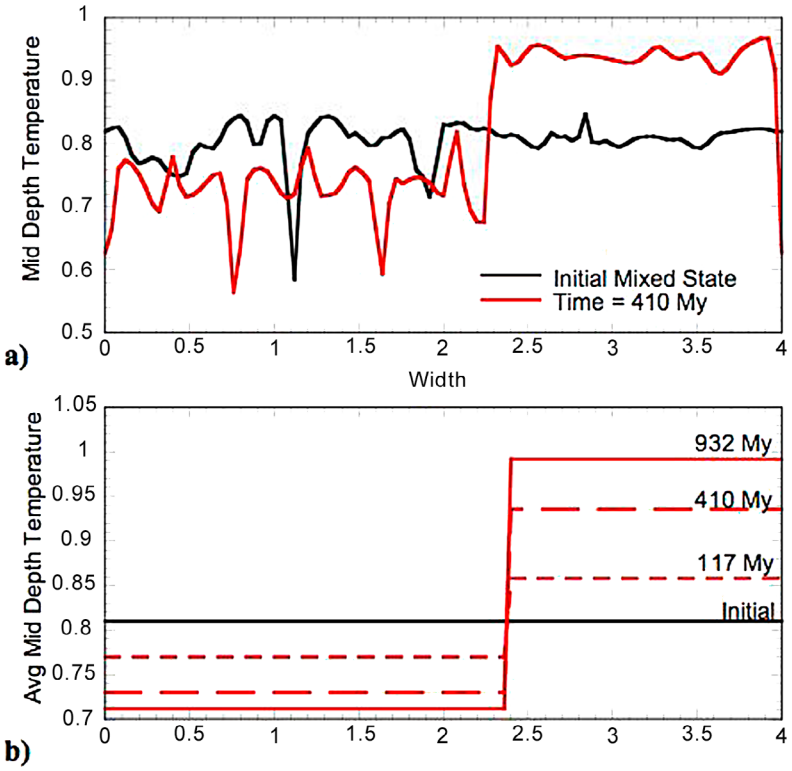

Figure 8. (a) Mid-mantle lateral temperature profiles from two points in the model evolution from Figure 7a. (b) Average sub-ocean and subcontinental mid-mantle temperature profiles from the model of Figure 7a.

cosity of the lower mantle provides added inhibition of thermal mixing in the isolated regime (compare the middle simulation of Figure 11a to the simulation of Figure 7b).

[24] The network model makes it clear that if continental and oceanic plate thickness are considered to be the same, then continental insulation will not be significant. Thus, models that prescribe the thickness of oceanic plates and set that thickness to be near that of continental plates should not produce significant insulation effects. For the present day Earth, the bulk of evidence points to an on average thicker thermal continental lithosphere relative to oceanic lithosphere [e.g., *Jordan*, 1981; *Jordan et al.*, 1989; *Niu et al.*, 2004; *Lee et al.*, 2005]. Under greater degrees of convective vigor, in the Earths past, the thickness of the oceanic thermal boundary layer (oceanic plates) should decrease faster than the continental plate thickness (due to the stabilizing effect of the buoyant chemical lithosphere, i.e., continental crust and depleted mantle). However, the effective resistance will also depend on the aspect ratio of convection cells in oceanic regions. This geometric effect appears as a free scaling constant in our theoretical scaling analysis (no theory we know of can predict aspect ratios, i.e., convection patterns, for even the simplest of situations). Laboratory experiments have shown that partially insulated convection, under stagnant lid conditions, can transition from a thermally well mixed to a thermally isolated state as the ratio of insulating area increases relative to the characteristic wavelength of convective flow [*Jellinek and Lenardic*, 2009].

[25] Prescribing low or zero heat flux boundary conditions over portions of a modeling domain, as a means to mimic continents, can provide a potential insulation effect [e.g., *Grigne et al.*, 2007; *Heron and Lowman*, 2010]. However, the level of mantle mixing in this approach differs from that of models with continental lithosphere immersed in the mantle. This is made clear by the simulations of Figure 12. Prescribing a supercontinent as a local boundary condition leads to a thermally well mixed state while the otherwise equivalent model with continental lithosphere leads to thermal isolation (Figure 12, top). The simulations in Figure 12 also highlight how mechanical conditions can affect internal mantle temperatures. The simulation with a rigid mechanical condition in the zero heat flux region (Figure 12, middle) leads to a greater average internal temperature than the case with a free

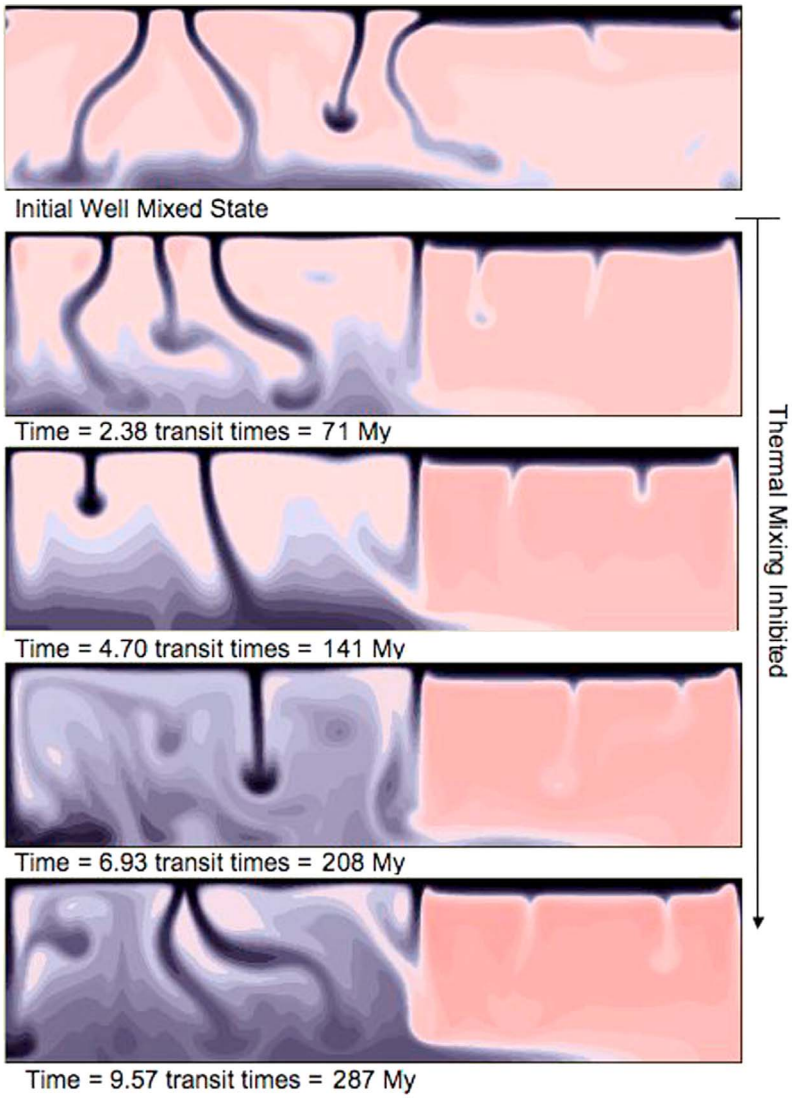

Figure 9. Temporal evolution of a purely internally heated numerical simulation that transitions from a thermally well mixed to a thermally isolated regime. The transition is initiated in the same manner as for the simulations of Figure 7a.

slip condition (Figure 12, bottom). This is in line with our scaling predictions (Appendix A). The rigid condition case does lead to a small amplitude thermal anomaly below the model continental region but it is very shallow. That is, unlike the simulations that model immersed continental lithosphere, the potential temperature of the bulk mantle below the supercontinent does not differ significantly from that below oceanic regions.

3. Laboratory Experiments

[26] Our results show that protracted strong subduction at the margins of a supercontinent can "short circuit" mantle stirring and give rise to persistent large lateral temperature variations. Collapse of this unstable regime, in response to continental breakup or as a consequence of the buoyancy forces related to these lateral temperature variations destabilizing the subduction, can lead to large-scale mantle overturning the form of which can be complicated. Resulting transient dynamics can have significant thermal effects in the oceanic and continental mantles, the observable implications for which we discuss in the subsequent section. An obvious question, however, is the robustness of this behavior. That is, is it a generic property of convecting systems with partial insulation. To this end we show results from a comparable set of laboratory experiments aimed at exploring this phenom-

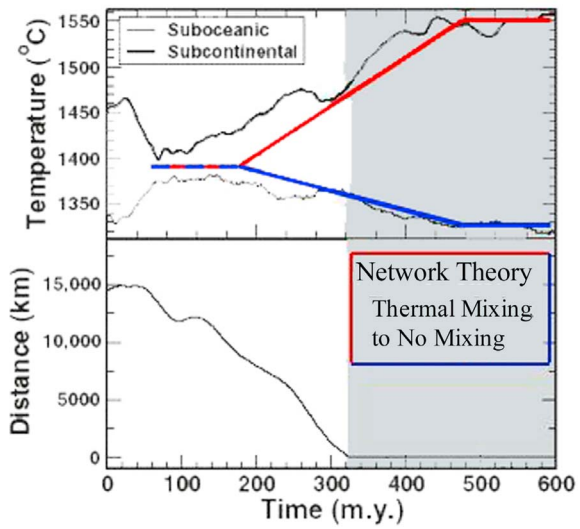

Figure 10. (top) Comparison of scaling theory predictions to the numerical simulation results of *Coltice et al.* [2007]. (bottom) The distance between two drifting continents over time. At distance moves to zero, a model supercontinent forms.

enon. We focus on key aspects of the evolving structure of the flow and the responses of the interior and basal temperature fields. As our numerical simulations focus on the effects of large continents, we restrict this discussion to an experiment with an insulating lid that initially covers approximately 49% of the cold surface. A complete discussion that investigates the effect of lid extent on these transient flows is the subject of an additional paper.

[27] A layer of corn syrup is heated from below with a resistance heater and cooled from above with a well-stirred layer of very low viscosity mineral oil (Figure 13a). Much like the Earth's mantle deforming in the diffusion creep limit, the corn syrup has a strongly temperature-dependent Newtonian viscosity of the form $\mu(T) = \mu_c \exp(-\gamma T)$, where $\gamma = 0.2 \pm 0.02°C^{-1}$ is the rheological temperature scale and the reference viscosity for the syrup $\mu_c = 12\ Pa - s$. Prior to the start of an experiment, a removable barrier constructed of stainless steel and low-conductivity nylon fabric is inserted at the interface between the oil and syrup to provide partial insulation at the cold boundary with a lateral extent that we can vary. Once started, each experiment is run to statistically steady conditions with partial insulation, quantitatively consistent with *Jellinek and Lenardic* [2009]. The plate is then carefully but quickly removed in such a way that no shear is imparted to the flow and the system is allowed to evolve through a transient thermal regime into a new and thermally well mixed steady state. With a lid covering 49% of the cold surface the effective Rayleigh number based on the average steady-state temperature difference from the hot boundary to the cold bath, a layer depth and fluid properties adjusted for the presence and insulating effects of the lid [*Jellinek and Lenardic*, 2009] and a viscosity based on the mean temperature of the system is 2×10^8.

[28] Consistent with *Jellinek and Lenardic* [2009], under the initial partially-insulated steady state conditions the heat flux is carried across the layer through a combination of large-scale overturning motions driven by strong, high viscosity cold plumes descending beneath the gap and by nearly isoviscous thermals rising primarily beneath the lid (Figure 13b). Episodic hot plumes rising through the cold downwelling are also observed and are qualitatively comparable to the "bursting" behavior reported by *Thayalan et al.* [2006] in numerical simulations. A key feature of this regime is that the flow maintains a large lateral interior temperature difference from the lid to the gap side (Figure 13a). Upon removal of the lid this lateral temperature difference becomes unstable and the gravitational potential energy is released as the cold fluid beneath the gap descends beneath rising hot fluid that was initially beneath the lid (Figures 13c and 13d). The arrival and spreading of this cold material perturbs the temperature at the hot boundary (Figure 14a) and "bulldozes" thermal boundary layer fluid, which causes both an increase in the frequency of plume formation [cf. *Robin et al.*, 2007] as well as a clustering in time of plume-forming events (Figures 14b and 14c). As the experiment progresses, the internal temperature of the system becomes uniform and a steady-state stagnant lid mode of convection is recovered. It is useful to note that consistent with the numerical simulations, the final internal temperature is the average of the initial lid and gap sides.

4. Discussion

[29] The numerical study of *O'Neill et al.* [2009] predicted minor heating below supercontinents relative to the very similar numerical study of *Coltice et al.* [2009]. The reason is now clear: The supercontinent drifting freely relative to the convecting mantle favored lateral thermal mixing in the simulations of *O'Neill et al.* [2009]. The simulations of *Heron and Lowman* [2010], which where used to argue for even smaller degrees of heating below

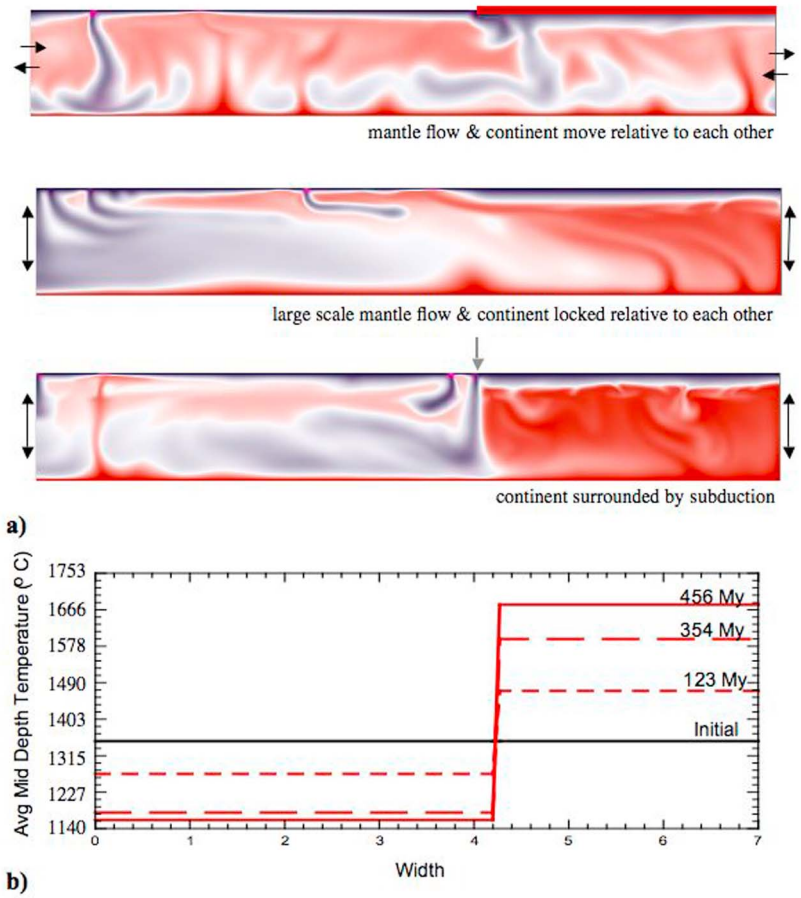

Figure 11. (a) Mantle convection simulations with 40% continental lithosphere of 0.05 thickness. Violet region in the oceanic lithosphere are failure zones (regions were convective stress reaches the material yield stress leading to the generation of concentrated zones of weakness). The surface Rayleigh number is 3×10^2, the temperature-dependence of viscosity is set by $\theta = 13.82$, the ratio of the internal to basal heating Rayleigh number is 3, and the lower mantle is 100 times more viscous than the upper mantle. (b) Average sub-ocean and subcontinental mid-mantle temperature profiles from a simulation that transitions from a thermally well mixed state (as per the top simulation in Figure 11a) to a thermally isolated state (as per the bottom simulation in Figure 11a). We have dimensionalized the mid-depth temperatures assuming a mantle potential temperature of 1350 C in the thermally well mixed state.

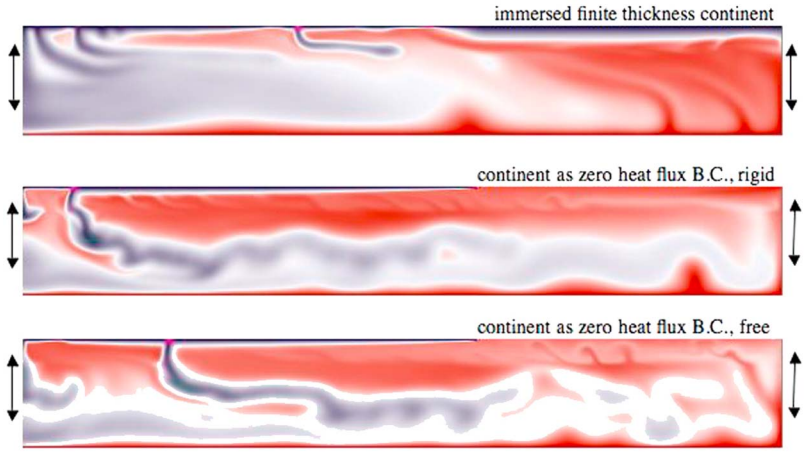

Figure 12. Comparison of a simulation that allows for finite thickness continents (as per Figure 11) to simulations that mimic the thermal effect of continents via a no heat flux surface boundary condition.

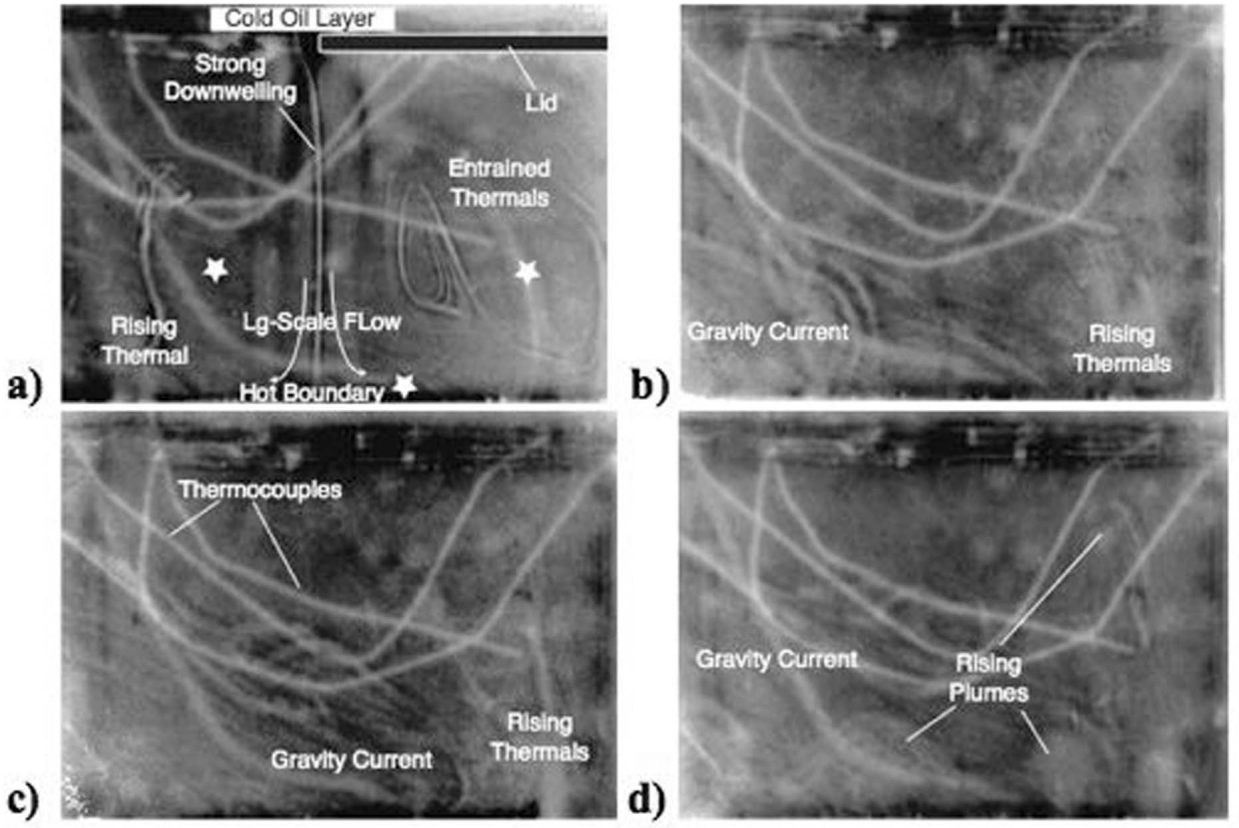

Figure 13. Time series of photographs showing the evolution from initially steady-state partially-insulated flow through the transient regime following lid removal. (a) Initial thermally isolated state (the stars show the location of thermal sensors). (b) Just after transition toward a thermally well mixed state is initiated. (c) Advancing basal gravity current from the cold 'suboceanic' region. (d) Cold gravity current has moved across the tank, initiating large plumes from the lower thermal boundary layer.

supercontinents, prescribed the thickness of oceanic and continental plates to be equivalent and modeled the thermal effect of continents via a surface boundary condition. Neither of these conditions favors the emergence of a thermal isolation regime, with a localized mantle insulation effect below a supercontinent, thus it was not observed.

[30] A crucial issue in determining whether or not thermal isolation can occur during a supercontinent episode is the extent of thermal mixing. In general, the mantle tends toward efficient thermal mixing within its interior. Isolation can occur but only under restrictive conditions. Consequently, our results do not imply that supercontinents will necessarily lead to heating events below themselves. A supercontinent can remain fixed at the Earths surface and lateral thermal mixing can still be efficient if there is large scale mantle flow relative to the continent. The fact that two distinct regimes can exist under identical parameter conditions shows the limitations of using purely numerical simulation based arguments to rule out a temperature increase below a supercontinent or to argue that its inevitable for all supercontinents. Both states are possible for the same mantle Rayleigh number, heating mode, rheology, continental thickness, and continental area. The difference between the two is largely one of mantle flow patterns relative to a supercontinent. For example, if the mantle flow configures itself to allow for subduction zones that encircle a supercontinent, then transition to a thermally isolated state can occur with an associated increase in temperature below a supercontinent. The degree to which isolation occurs can still be variable depending on the how continuous peripheral subduction is and on how long the configuration lasts (Figure 8b).

[31] Mapping the two end member states leads to predictions about the effects that would occur during transitions between them. In particular, we have highlighted that any transition will effect not only the mantle below a supercontinent but also the mantle below oceanic regions. The added predic-

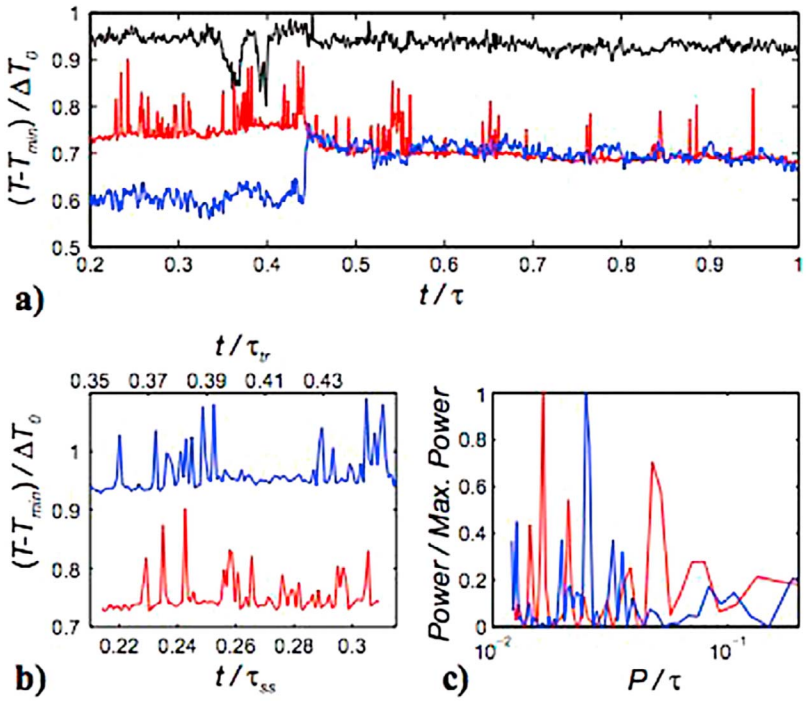

Figure 14. (a) Time series of temperatures from near the hot boundary (black) and the flow interior beneath the lid (red) and the gap (blue). (b and c) Time series of internal temperature and corresponding power spectra from the lid side only showing data for the partial-lid regime before the transient (red, bottom time axis) and for the transient following lid removal (blue, top time axis). The temperatures for the transient have been increased by 0.2 so that they can be easily compared with the pre-transient data on the same plot. The enhanced frequency of plume formation and the clustering in time of these instabilities during the transient is correlated in time with the spread of cold fluid from the gap side. Time is normalized to the thermal diffusion time across the tank, ΔT_0 is the average temperature drop from the hot boundary to the cold oil bath and P is the period for plume formation.

tions that come with this analysis can be compared against observations to determine if insulation-driven, supercontinent heating events did occur (we use the term "insulation-driven" to distinguish this from the situation of a local temperature increase due to plumes rising below a supercontinent [*Zhong et al.*, 2007; *Zhang et al.*, 2010; *Heron and Lowman*, 2010] - the plume scenario would not be associated with major changes in the potential temperature below oceanic domains). Comparing the full range of model predictions to observations from distinct supercontinent episodes goes beyond the scope of this paper. We can, at this stage, offer some comments regarding the general observational "pattern" or "fingerprint" expected from the evolution through mixing/isolation/mixing regimes.

[32] There are two key characteristics of an isolation regime that have not been highlighted to date: A drop in oceanic potential temperature and a corresponding increase in oceanic mantle viscosity. The reduction in temperature has distinct effects at the top and bottom of the mantle. At the top of the mantle, the drop in oceanic potential temperature will lead to a corresponding drop in sea level, with the magnitude depending on the time scale over which an isolated state is maintained. The results of Figure 11b can be used to give a sense of the potential magnitude of sea level changes. The change in oceanic potential temperature for isolation lasting between 123–354 Myr is 88–175 C, assuming a reference mantle potential temperature of 1350 C in the thermally well mixed state. For this range of oceanic mantle potential temperature changes, the sea level change, associated only with thermal isostasy, is in the range of 100–200 meters. A drop in oceanic potential temperature will also lead to a reduction in the rate of mantle melting, crustal production, and outgassing at ridges, which modulates climate. When the increase in oceanic mantle viscosity is considered, which reduces the rate of mantle stirring and thus melting at both ridges and arcs, these effects are enhanced. At the bottom of the mantle, the core-mantle boundary (CMB) heat flux becomes highly asymmetric. The effect on the geodynamo would depend on whether

the supercontinent is equatorially located. If it is, then this could drive a decline in magnetic reversal frequency [*Olson et al.*, 2010]. The temperature increase below the supercontinent, which extends to the deep mantle (Figure 11a) would cause a local decline in CMB heat flux and an associated change in the nature of subcontinental mantle plumes. The lower viscosity variations across the boundary layer, due to local mantle heating, would favor isoviscous thermal as opposed to relatively low viscosity plumes. The decreased temperature below oceanic domains, and the associated increase in the viscosity contrast across the lower thermal boundary layer, would favor strong cavity plumes [*Lenardic and Kaula*, 1994; *Jellinek et al.*, 2002; *Thayalan et al.*, 2006].

[33] Transitioning from an isolated to a thermally well mixed state would lead to a rise in sea level. The lateral temperature gradient that would be unleashed during transition would contribute to a pulse of enhanced convective vigor, oceanic plate overturn, and mantle degassing, which would favor a warm climate. The changes in CMB flux during the transition, in particular the oceanic cold front that would spread below the dispersing supercontinent, would trigger a burst of increased mantle plume activity (Figure 14). Thus, an increase in large igneous provinces would be expected following continental dispersal (delayed by the transit time of plumes across the mantle). After the initial pulse associated with the mixing of the subcontinental warm "front" and the oceanic cold "front", a transient configuration of anomalously warm upper mantle over anomalously cold lower mantle would be established. This stable density configuration, together with the initial plume burst thinning the thermal boundary layer above the CMB, would lead to a period of relatively low CMB heat flux. The low global CMB heat flux, over the duration of this transient thermal layering, would favor reduced magnetic field intensity and reversal frequency [*Olson et al.*, 2010]. The horizontal temperature gradient would provide an added plate driving force, the direction of which would tend to cause dispersing continents to override subduction zones. The would favor a globally synchronous period of compression at the leading edge of continents together with enhanced continental arc volcanism.

[34] The degree to which the effects above would occur depends on the time scale over which isolation is maintained and there is no reason this should be the same for all supercontinent episodes, just as there is no a priori reason that isolation should occur at all for all supercontinent episodes. That said, the number of specific predictions, and the links between them, are promising for comparison to observational data. A future study will focus on simulations that transition between the two dynamic states and compare model predictions to available data over the Earth's last episode of supercontinent assembly and dispersal to determine if a supercontinent heating event did occur and, if so, the degree to which it effected the Earth system.

5. Conclusion

[35] If the thickness and thermal properties of continental lithosphere are such that the resistance to mantle heat transfer is greater below continents then oceans, then continents can insulate the convecting mantle. The insulating potential does not depend on whether continents are dispersed and drifting relative to each other or if they are amalgamated into a single supercontinent. In the former state, the insulating effect of continental lithosphere is communicated to the entire mantle via lateral thermal mixing between suboceanic and subcontinental domains. Thus, the potential temperature of the entire mantle is greater than it would be without insulating continents. During a supercontinent state the mantle can remain thermally well mixed if the supercontinent drifts relative to the large scale pattern of mantle flow. Thus, a supercontinent event will not necessarily be associated with a local temperature increase below the supercontinent. If the supercontinent becomes rimmed by peripheral subduction zones, then thermal communication below the subcontinental and suboceanic domains can be cut-off. This allows the insulating effect of continental lithosphere to become localized. The mantle potential temperature below suboceanic domains drops as the insulating effect of continental lithosphere is no longer communicated to entire mantle. The potential temperature below the supercontinent increases in a manner that leads the bulk average mantle temperature to remain unchanged (i.e. the temperature decrease below suboceanic domains balances the increase below the supercontinent).

[36] Our analysis leads to the conclusion that if a rise in mantle potential temperature did occur below supercontinents in the Earth's past, then the potential temperature of the suboceanic mantle would have decreased. The change in mantle thermal state would result from the insulating effect of continental lithosphere no longer being communicated to the suboceanic mantle via thermal

mantle mixing. The dependence on thermal mixing means that a significant increase in mantle temperature below a supercontinent can occur on an advective time scale (i.e. 10^8 years). This removes objections to the viability of super-continental thermal events based on the idea that they would occur on a time scale set by the rate of internal heat generation (which would exceed the time over which supercontinents remain assembled). The connection to the oceanic domain also leads to a greater range of predictions that can be used to determine if supercontinent thermal events did or did not occur in the Earth's past. A temperature drop in the suboceanic mantle would lead to an increase in mantle viscosity and an associated decrease in the velocity of oceanic plates. This, in turn, would tend to decrease mantle degassing from ridges and arcs. During continental breakup, the large lateral temperature variation that would have developed from the subcontinental to the suboceanic mantle would drive a transient burst of enhanced convective vigor with enhanced ridge and arc activity. The direction of flow induced by the temperature gradient would favor continents over-riding subduction zones leading to a pulse of enhanced continental arc activity.

Appendix A: Scaling Theory

[37] The system we address, the basis of our theoretical approach, and the simplifications we will make are shown in Figure 1. The full problem is simply stated: Develop a heat flow scaling theory for mantle convection interacting with continents. Despite the simplicity of statement, the full problem, allowing for all the potential complexities of the solid Earth system, is associated with an extremely large parameter space. We proceed by exploring a simplified system that retains several of the key elements of the full problem (Figure 1b). We focus first on the connection between stable continental lithosphere and the active mantle sublayer that forms below it. From there we link this thermal path to a resistance component associated with oceanic lithosphere. For a thermally well mixed state, the link involves defining a composite thermal resistance and developing a criteria that relates the driving temperature drop to the percentage of the system covered by the continental component. For the case of poor lateral mixing (the thermally isolated state), the link is simpler as the global heat flux will be a weighted average of cases with and without a continental lid.

A1. Full Continental Lid Theory

[38] We consider the system of Figure 1b in the limit where the convecting mantle is bounded uniformly by a conducting lid of thickness d. The lid imposes a rigid mechanical condition on the convecting mantle below. The temperatures at the system top, T_s, and base, T_b, are constant. The average temperature at the continental lid base, T_c, is an unknown to be solved for. The thermal conductivity of the continental lid and mantle are given by K_c and K_m, respectively.

[39] Convective vigor in the mantle depends on an effective Rayleigh number given by

$$Ra_{\text{eff}} = \frac{\rho_0 g \alpha (T_b - T_c)(D-d)^3}{\mu \kappa} \tag{A1}$$

where ρ_0 is the reference density of the fluid, g is gravitational acceleration, α is the thermal expansion coefficient of the fluid, μ is the fluid viscosity, and κ is the fluid thermal diffusivity. As it depends on T_c, Ra_{eff} is not known a priori. Thus, a more standard Rayleigh number will be useful and it is defined as

$$Ra = \frac{\rho_0 g \alpha \Delta T D^3}{\mu \kappa} \tag{A2}$$

where $\Delta T = T_b - T_s$. The two Rayleigh numbers are related by

$$Ra_{\text{eff}} = \frac{(T_b - T_c)}{\Delta T}(1 - d/D)^3 Ra. \tag{A3}$$

[40] We assume thermal equilibrium has been reached. Thus, the average heat flux into the base of the lid, q_c, is equal to the average surface heat flux. We can express q_c as

$$q_c = K_c \frac{T_c - T_s}{d}. \tag{A4}$$

[41] We assume that a nearly linear thermal gradient holds across the active upper thermal boundary layer of the mantle. The average thickness of this layer is denoted by δ_c. The average temperature drop across it is $T_{ic} - T_c$, where T_{ic} is the temperature of the thermally well-mixed interior. The mantle heat flux, q_c, can now be written as

$$q_c = K_m \frac{T_{ic} - T_c}{\delta_c}. \tag{A5}$$

Equating equations (A4) and (A5) provides an expression for δ_c given by

$$\delta = \frac{(T_{ic} - T_c)K_m d}{(T_c - T_s)K_c}. \quad \text{(A6)}$$

[42] We introduce a local boundary layer Rayleigh number, Ra_{δ_c}, given by

$$Ra_{\delta_c} = \frac{{\delta_c}^3 (T_{ic} - T_c)}{D^3 \Delta T} Ra_{\text{eff}}. \quad \text{(A7)}$$

and consider it to remain near a constant value, Ra_{crit} [*Howard*, 1966]. The critical Rayleigh number for the onset of convection is $\approx 10^3$ for a range of boundary conditions [*Sparrow et al.*, 1964]. However, the local boundary layer Rayleigh number can differ from the critical Rayleigh number for convective onset [*Sotin and Labrosse*, 1999]. To allow for this we consider $Ra_\delta = a_1 10^3$ where a_1 is a scaling constant. This leads to a second expression for δ_c given by

$${\delta_c}^3 = \frac{a_1 10^3 D^3 \Delta T}{(T_{ic} - T_c) Ra_{\text{eff}}}. \quad \text{(A8)}$$

[43] We close the problem by considering a symmetric temperature profile to hold in the convecting mantle so that

$$T_{ic} = \frac{T_b + T_c}{2}. \quad \text{(A9)}$$

This assumes that the thermal boundary layer that forms at the mantle base will be of the same thickness as the active upper thermal boundary layer of the mantle. This symmetry relies on the mechanical condition at the top and the base of the convecting portion of the mantle being of the same type. We return to this issue shortly.

[44] Equations (A3), (A6), (A8), and (A9) can be used to derive an expression for T_c. We simplify the expression by nondimensionalizing the system using D as the length scale, K_m as the conductivity scale, and ΔT as the temperature scale (this allows us to set the nondimensional temperature at the system surface and base to zero and one, respectively; it also means that the heat flux given by equation (A4) can be equated to the Nusselt number, Nu). The final expression is

$$\frac{(1 - T_c)^5}{T_c^3} = \frac{a_1 16000 K_c^3}{(d - d^2)^3 Ra}. \quad \text{(A10)}$$

Together with equation (A4), this allows us to solve for the surface heat flux as a function of Ra, d, and K_c.

[45] We now consider a free slip mechanical condition at the mantle base. The bulk of the theoretical framework carries over. The only change is associated with the fact that the critical boundary layer Rayleigh number depends on the mechanical condition felt by the boundary layer [*Howard*, 1966; *Sotin and Labrosse*, 1999]. The symmetry condition of equation (A9) is valid if the thermal sublayer below the continental lid and the thermal layer at the base of the mantle having equal thicknesses. The mechanical asymmetry associated with a free slip base means that the critical boundary layer Rayleigh numbers for the upper active thermal boundary layer and for the lower thermal boundary layer will differ. Therefore their equilibrium thicknesses will also differ and a symmetric temperature profile will not exist within the convecting mantle layer.

[46] We first consider the no lid limit with a rigid surface and a free slip base. The temperature drops across the upper and lower boundary layers are denoted by ΔT_u and ΔT_l, respectively. Their thicknesses are denoted by δ_u and δ_l and their associated boundary layer Rayleigh numbers by Ra_{δ_u} and Ra_{δ_l}. Boundary layer thickness scales with the boundary layer Rayleigh number to the $-1/3$ power. In equilibrium the heat flow rate across the boundary layers is equal. Thus,

$$\frac{\Delta T_u}{\Delta T_l} = b_1 \frac{Ra_{\delta_u}}{Ra_{\delta_u}} \quad \text{(A11)}$$

where b_1 is a scaling constant. The boundary layer Rayleigh numbers are assumed to remain near a critical value proportional to the critical Rayleigh number for the convective onset [*Howard*, 1966]. This leads to

$$\Delta T_u / \Delta T_l = b_1 [1707/657]^{1/3} \quad \text{(A12)}$$

where we have used critical Rayleigh numbers for rigid and free boundaries [*Sparrow et al.*, 1964]. The scaling constant, b_1, should be near unity.

[47] We ran a series of numerical simulations to test the above. For an Ra range of 10^4–10^9 the bulk internal temperature approached 0.64 for the higher Ra cases (i.e., $Ra = 10^6$–10^9). This sets the scaling constant b_1 to 1.3. We adopt this value and assume that the boundary layer asymmetry described by equation (A12) will continue to hold for the active upper and lower boundary layers in the situation

where a lid is present above the convecting fluid. This leads to an expression for the bulk internal temperature given by

$$T_{ic} = 0.64 + 0.36T_c. \tag{A13}$$

This expression replaces equation (A9).

[48] Accounting for the change noted above, and retaining all other aspects of the previous subsection, allows derive an expression for T_c for the case of a free slip base. The expression is given by

$$\frac{(1-T_c)^5}{T_c^3} = \frac{a_1 5960.46 K_c^3}{(d-d^2)^3 Ra}. \tag{A14}$$

A2. Partial Continental Lid Theory

[49] We now consider convection below a conducting continental lid of finite lateral extent, L (Figure 1b). We non-dimensionalize the system so that L is the continental extent relative to the system extent.

[50] The average total system heat flux, q_t, can be expressed as the product of the average temperature drop across the composite upper boundary layer, ΔT_t, divided by its effective thermal resistance, R_t. That is,

$$q_t = \frac{\Delta T_t}{R_t} \tag{A15}$$

Similarly, the heat flux for the end-member cases of a system completely covered by or completely free of continents can be expressed as

$$q_c = \frac{\Delta T_c}{R_c} \tag{A16}$$

and

$$q_o = \frac{\Delta T_o}{R_o} \tag{A17}$$

respectively.

[51] For the composite network, we consider the effective local resistance of each separate heat flow path to decrease as the non-dimensional width of the path increases and we consider resistances to add in parallel. Thus, the inverse of total thermal network resistance is

$$R_t^{-1} = R_c^{-1} L + R_o^{-1}(1-L) \tag{A18}$$

This allows us to express the total system heat flux as

$$q_t = (1-L)q_o \frac{\Delta T_t}{\Delta T_o} + Lq_c \frac{\Delta T_t}{\Delta T_c}. \tag{A19}$$

[52] For $L = 1$ we must recover the scaling results of the full lid subsection. Thus, q_c in equation (A19) must be the same as the heat flux determined from equations (A4) and (A10). The term $\frac{\Delta T_t}{\Delta T_c}$ is a weighting factor that accounts for the fact that the continental heat flux for the case of a partial continental lid will differ from the case of a full lid due to the fact that the average internal temperature depends on continental extent. We will at this stage assume thorough thermal mixing within the mantle to derive an expression for this dependence. For thorough mixing, the average internal temperature of the entire system, T_{it}, will be a weighted average of the internal temperature for the case of complete continental coverage, T_{ic}, and for the no continent case, T_{io}. That is,

$$T_{it} = (1-L)T_{io} + LT_{ic}. \tag{A20}$$

[53] For the no continent case, the average internal temperature will be one half of the surface plus the base temperature. This leads to an expression for the total system heat flux given by

$$q_t = (1-L)q_o[(1-L) + 2LT_{ic}] + Lq_c\left[\frac{(1-L)}{2T_{ic}} + L\right]. \tag{A21}$$

Together with equations (A10), (A9), and (A4) this closes the problem for the case of a partial lid if it is assumed that q_o is known function of Ra. This amounts to saying that a theoretical scaling already exists for free thermal convection between isothermal boundaries, i.e., for the classic Rayleigh-Bénard problem. For consistency, this scaling should be of the same form as would result from considering our full continental lid scaling in the limit of the conducting lid thickness going to zero. That is, if equation (A8) is taken as the stability criterion for the thermal boundary layer that forms below the conducting lid, then q_o must scale as $Ra^{1/3}$ [*Howard*, 1966]. We will thus consider q_o to scale as $Ra^{1/3}$ with the scaling constant determined through direct comparison to numerical simulation results. The global heat flux can then be calculated for the partial lid case as a function of d, L, K_L, and Ra.

[54] Along with global heat flux, local average heat fluxes can also be determined. In equation (A21), the term $q_o[(1-L) + 2LT_{ic}]$ represents the average heat flux in the oceanic zone while the term $q_c[\frac{(1-L)}{2T_{ic}} + L]$ represents the average subcontinental mantle heat flux. This latter term, together with the lids thickness and thermal conductivity allows

one to solve for the average temperature at the base of the continental lid.

[55] Our partial lid scalings thus far have assumed thorough thermal mixing. This assumption may break down depending on boundary conditions and parameter values. We can anticipate this potential by considering the other extreme case of no thermal mixing. For that case, the total system heat flux can be expressed as an area weighted average of the heat flux from each end-member, i.e.,

$$q_{tnm} = (1 - L)q_o + Lq_c \tag{A22}$$

where the added subscript *nm* makes it clear that this holds for the case of no thermal mixing.

Appendix B: Numerical Simulations

[56] The simulations discussed used the CITCOM finite element [*Moresi and Solomatov*, 1995] to solve the equations of thermal convection, allowing for continental lids. The non-dimensional system of equations are given by:

$$\partial_i u_i = 0 \tag{B1}$$

$$\partial_j \left[2\mu\left(T, \tau_{yield}, D\right)\epsilon_{ij}\right] = \partial_i p + RaT\hat{k} \tag{B2}$$

$$\partial_t T + u_i \partial_i T = \partial_i^2 T + H \tag{B3}$$

$$\rho = [1 - \alpha(T - T_0)] \tag{B4}$$

where

$$Ra = \frac{\rho_0 g \alpha \Delta T D^3}{\mu \kappa}$$

$$H = \frac{Ra_i}{Ra} = \frac{\rho_0 Q d^2}{\Delta T K_0}$$

and u_i is the velocity vector, $\mu(T, C, \tau_{yield}, D)$ is a viscosity function, T is temperature, τ_{yield} is a material yield stress, D is the second invariant of the strain rate tensor, ϵ_{ij} is the strain rate tensor, p is pressure, Ra is the Rayleigh number, $\hat{k}$ is the vertical unit vector, ρ is the mantle density, α is the coefficient of thermal expansion, g is the gravitational acceleration, ΔT is the temperature drop across the system, D is the system depth, κ is thermal diffusivity, H is the ratio of the thermal Rayleigh number defined for internal heating to that defined for bottom heating, and Q is internal heat generation per unit mass. Equation (B1) is the mass conservation equation assuming incompressible material, equation (B2) is the momentum conservation equation for creeping flow, equation (B3) is the energy conservation equation assuming no internal or frictional heating, and equation (B4) is the linearized equation of state. Two means of representing a conducting lid where tested and each lead to equivalent results. The first set the viscosity to a relatively high value in the lid region while the second prescribed zero velocity conditions in the lid region.

[57] For temperature and yield stress dependent simulations, the viscosity function follows that of *Moresi and Solomatov* [1998]. The flow law has two branches. Mantle rheology remains on a temperature-dependent viscous branch for stresses below a specified yield stress, τ_{yield}. Along this viscous branch, diffusion creep is considered to be the deformation mechanism and the viscosity function is given by:

$$\mu_{creep} = A \exp[-\theta T] \tag{B5}$$

where A and θ are material parameters. For stresses above τ_{yield}, the flow law switches to a depth-dependent plastic branch. The yield criterion is defined by:

$$\tau_{yield} = \tau_0 + \tau_1 z \tag{B6}$$

where τ_0 is the yield stress at zero hydrostatic pressure, τ_1 is the slope of the linear yield curve, and z is depth. The non-linear, effective viscosity along the plastic deformation branch is given by

$$\mu_{plastic} = \frac{\tau_{yield}}{D} \tag{B7}$$

where D is the second strain-rate invariant and the dependence on C indicates that different components can have different yield stress values.

Acknowledgments

[58] This research was supported by NSF grants EAR-0448871 and EAR-0944156. AMJ was supported by the Canadian Institute for Advanced Research and NSERC. Thanks to Shijie Zhong and Nicolas Coltice for constructive reviews.

References

Anderson, D. L. (1982), Hotspots, polar wander, Mesozoic convection and the geoid, *Nature*, *297*, 391–393.

Boyd, F. R., J. J. Gurney, and S. H. Richardson (1985), Evidence for a 150–200 km thick Archean lithosphere from diamond inclusion thermobarometry, *Nature*, *315*, 387–389.

Bunge, H. P., M. A. Richards, and J. R. Baumgardner (1996), Effect of depth-dependent viscosity of the planform of mantle convection, *Nature*, *379*, 436–438.

Busse, F. H. (1978), A model of time-periodic mantle flow, *Geophys. J. R. Astron. Soc.*, *52*, 1–12.

Busse, F. H., M. A. Richards, and A. Lenardic (2006), A simple model of high Prandtl and high Rayleigh number convection bounded by thin low viscosity layers, *Geophys. J. Int.*, *164*, 160–167.

Coltice, N., B. R. Phillips, H. Bertrand, Y. Ricard, and P. Rey (2007), Global warming of the mantle at the origin of flood basalts over supercontinents, *Geology*, *35*, 391–394.

Coltice, N., H. Bertrand, P. Rey, F. Jourdan, B. R. Phillips, and Y. Ricard (2009), Global warming of the mantle beneath continents back to the Archean, *Gondwana Res.*, *15*, 254–266, doi:10.1016/j.gr.2008.10.001.

Cooper, C. M., A. Lenardic, and L.-N. Moresi (2004), The thermal structure of stable continental lithosphere within a dynamic mantle, *Earth Planet. Sci. Lett.*, *222*, 807–817.

Cooper, C. M., A. Lenardic, and L. Moresi (2006), Effects of continental insulation and the partitioning of heat producing elements on the Earth's heat loss, *Geophys. Res. Lett.*, *33*, L13313, doi:10.1029/2006GL026291.

Grigne, C., S. Labrosse, and P. J. Tackley (2007), Convection under a lid of finite conductivity: Heat flux scaling and application to continents, *J. Geophys. Res.*, *112*, B08402, doi:10.1029/2005JB004192.

Guillou, L., and C. Jaupart (1995), On the effect of continents on mantle convection, *J. Geophys. Res.*, *100*, 24217–24238.

Gurnis, M. (1988), Large scale mantle convection and the aggregation and dispersal of supercontinents, *Nature*, *332*, 695–699.

Heron, P. J., and J. P. Lowman (2010), Thermal response of the mantle following the formation of a "super-plate," Geophys. Res. Lett., *37*, L22302, doi:10.1029/2010GL045136.

Hoink, T., and A. Lenardic (2008), Three-dimensional mantle convection simulations with a low-viscosity asthenosphere and the relationship between heat flow and the horizontal length scale of convection, *Geophys. Res. Lett.*, *35*, L10303, doi:10.1029/2008GL033391.

Hoink, T., and A. Lenardic (2010), Long wavelength convection, poiseuille-couette flow in the low-viscosity asthenosphere and the strength of plate margins, *Geophys. J. Int.*, *180*, 23–33.

Howard, L. N. (1966), Convection at high Rayleigh number, in *Applied Mechanics, Proceedings of the 11th Congress of Applied Mechanics, Munich (Germany)*, edited by H. Gortler, pp. 1109–1115, Springer, Berlin.

Jellinek, A. M., and A. Lenardic (2009), Effects of spatially varying roof cooling on Rayleigh-Benard convection in a fluid with temperature-dependent viscosity, *J. Fluid Mech.*, *629*, 109–137, doi:10.1017/S0022112009006260.

Jellinek, A. M., A. Lenardic, and M. Manga (2002), The influence of interior mantle temperature on the structure of plumes: Heads for Venus, tails for the Earth, *Geophys. Res. Lett.*, *29*(11), 1532, doi:10.1029/2001GL014624.

Jordan, T. H. (1981), Continents as a chemical boundary layer, *Philos. Trans. R. Soc. London, Ser. A*, *301*, 359–373.

Jordan, T. H., A. L. Lerner-Lam, and K. C. Craeger (1989), Seismic imaging of boundary layers and deep mantle convection, in *Mantle Convection: Plate Tectonics and Global Dynamics*, edited by W. R. Peltier, pp. 97–201, Gordon and Breach, New York.

Lee, C. A., A. Lenardic, C. M. Cooper, F. Niu, and A. Levander (2005), The role of chemical boundary layers in regulating the thickness of continental and oceanic thermal boundary layers, *Earth Planet. Sci. Lett.*, *230*, 379–395.

Lenardic, A., and W. M. Kaula (1994), Tectonic plates, D″ thermal structure, and the nature of mantle plumes, *J. Geophys. Res.*, *99*, 15697–15708.

Lenardic, A., and W. M. Kaula (1995), Mantle dynamics and the heat flow into the Earth's continents, *Nature*, *378*, 709–711.

Lenardic, A., and W. M. Kaula (1996), Near surface thermal/chemical boundary layer convection at infinite Prandtl number: Two-dimensional numerical experiments, *Geophys. J. Int.*, *126*, 689–711.

Lenardic, A., and L.-N. Moresi (2001), Heat flux scalings for mantle convection below a conducting lid: Resolving seemingly inconsistent modeling results regarding continental heat flow, *Geophys. Res. Lett.*, *28*, 1311–1314.

Lenardic, A., and L.-N. Moresi (2003), Thermal convection below a conducting lid of variable extent: Heat flow scalings and two-dimensional, infinite Prandtl number numerical simulations, *Phys. Fluids*, *15*, 455–466.

Lenardic, A., L.-N. Moresi, A. M. Jellinek, and M. Manga (2005), Continental insulation, mantle cooling, and the surface area of oceans and continents, *Earth Planet. Sci. Lett.*, *234*, 317–333.

Lenardic, A., M. A. Richards, and F. H. Busse (2006), Depth-dependent rheology and the horizontal length scale of mantle convection, *J. Geophys. Res.*, *111*, B07404, doi:10.1029/2005JB003639.

Lowman, J. P., and C. W. Gable (1999), Thermal evolution of the mantle following continental aggregation in 3D convection models, *Geophys. Res. Lett.*, *26*, 2649–2652.

Lowman, J. P., and G. T. Jarvis (1993), Mantle convection flow reversals due to continental collisions, *Geophys. Res. Lett.*, *20*, 2087–2090.

Lowman, J. P., and G. T. Jarvis (1995), Mantle convection models of continental collision and breakup incorporating finite thickness plates, *Phys. Earth Planet. Inter.*, *88*, 53–68.

Moresi, L.-N., and V. S. Solomatov (1995), Numerical investigations of 2D convection with extremely large viscosity variations, *Phys. Fluids*, *7*, 2154–2162.

Moresi, L.-N., and V. S. Solomatov (1998), Mantle convection with a brittle lithosphere: Thoughts on the global styles of the Earth and Venus, *Geophys. J. Int.*, *133*, 669–682.

Morgan, P., and J. H. Sass (1984), Thermal regime of the continental lithosphere, *J. Geodyn.*, *1*, 143–166.

Niu, F., A. Levander, C. M. Cooper, C. A. Lee, A. Lenardic, and D. E. James (2004), Seismic constraints on the depth and composition of the mantle keel beneath the Kaapvaal craton, *Earth Planet. Sci. Lett.*, *224*, 337–346.

Olson, P. L., R. S. Coe, P. E. Driscoll, G. A. Glatzmaier, and P. H. Roberts (2010), Geodynamo reversal frequency and heterogeneous core-mantle boundary heat flow, *Phys. Earth Planet. Inter.*, *180*, 66–79.

O'Neill, C., A. Lenardic, A. M. Jellinek, and L. Moresi (2009), Influence of supercontinents on deep mantle flow, *Gondwana Res.*, *15*, 276–287.

Parsons, B., and D. P. McKenzie (1978), Mantle convection and the thermal structure of the plates, *J. Geophys. Res.*, *83*, 4485–4496.

Parsons, B., and J. G. Sclater (1977), An analysis of the variation of ocean floor bathymetry and heat flow with age, *J. Geophys. Res.*, *82*, 803–827.

Pekeris, C. L. (1935), Thermal convection in the interior of the Earth, *Mon. Not. R. Astron. Soc., Geophys. Suppl.*, *3*, 343–367.

Phillips, B. R., and N. Coltice (2010), Temperature beneath continents as a function of continental cover and convective wavelength, *J. Geophys. Res.*, *115*, B04408, doi:10.1029/2009JB006600.

Pollack, H. N., and D. S. Chapman (1977), On the regional variation of heat flow, geotherms, and the thickness of the lithosphere, *Tectonophysics*, *38*, 279–296.

Robin, C. M. I., A. M. Jellinek, V. Thayalan, and A. Lenardic (2007), Transient regimes in Benard convection in a fluid with a temperature-dependent viscosity and imposed large-scale stirring: Applications to Venus, *Earth Planet. Sci.Lett.*, *256*, 100–119.

Rudnick, R. L., W. F. McDonough, and R. J. O'Connell (1998), Thermal structure, thickness and composition of continental lithosphere, *Chem. Geol.*, *145*, 395–411.

Sotin, C., and S. Labrosse (1999), Three-dimensional thermal convection in an iso-viscous, infinite Prandtl number fluid heated from within and from below: Applications to the transfer of heat through planetary mantles, *Phys. Earth Planet. Inter.*, *112*, 171–190.

Sparrow, E. M., R. J. Goldstein, and V. K. Jonsson (1964), Thermal instability in a horizontal fluid layer: Effect of boundary condition and nonlinear temperature profile, *J. Fluid Mech.*, *18*, 513–528.

Stein, C. A., and S. Stein (1992), A model for the global variation in oceanic depth and heat flow with lithospheric age, *Nature*, *359*, 123–129.

Thayalan, V., A. M. Jellinek, and A. Lenardic (2006), Recycling the lid: Effects of subduction and stirring on lower boundary layer dynamics in bottom-heated planetary mantle convection, *Geophys. Res. Lett.*, *33*, L20318, doi:10.1029/2006GL027668.

Turcotte, D. L., and E. R. Oxburgh (1967), Finite amplitude convection cells and continental drift, *J. Fluid Mech.*, *28*, 29–42.

Turcotte, D. L., and G. Schubert (1982), *Geodynamics: Applications of Continuum Physics to Geological Problems*, 450 pp., John Wiley, New York.

Whitehead, J. A. (1972), Moving heaters as a model of continental drift, *Phys. Earth Planet. Inter.*, *5*, 199–212.

Zhang, N., S. J. Zhong, W. Leng, and Z. X. Li (2010), A model for the evolution of the Earth's mantle structure since the Early Paleozoic, *J. Geophys. Res.*, *115*, B06401, doi:10.1029/2009JB006896.

Zhong, S., and M. Gurnis (1993), Dynamic feedback between a continent-like raft and thermal convection, *Geophys. Res. Lett.*, *98*, 12219–12232.

Zhong, S., M. T. Zuber, L. Moresi, and M. Gurnis (2000), Role of temperature-dependent viscosity and surface plates in spherical shell models of mantle convections, *J. Geophys. Res.*, *105*, 11063–11082.

Zhong, S. J., N. Zhang, Z. X. Li, and J. H. Roberts (2007), Supercontinent cycles, true polar wander, and very long-wavelength mantle convection, *Earth Planet. Sci. Lett.*, *261*, 551–564.